Supramolecular photocatalysis: combining confinement and non-covalent interactions to control light initiated reactions

Nandini Vallavoju and J. Sivaguru*

Using non-bonding interactions to control photochemical reactions requires an understanding of not only thermodynamics and kinetics of ground state and excited state processes but also the intricate interactions that dictate the dynamics within the system of interest. This review is geared towards a conceptual understanding of how one can control the reactivity and selectivity in the excited state by employing confinement and non-covalent interactions. Photochemical reactivity of organic molecules within confined containers and organized assemblies as well as organic templates that interact through H-bonding and/or cation–carbonyl/cation–π interactions is reviewed with an eye towards understanding supramolecular effects and photocatalysis.

Key learning points

- Understanding host–guest interactions
- Directing photoreactivity through confinement
- Controlling reactivity and selectivity in light initiated reactions through hydrogen bonding interactions
- Supramolecular effects – understanding photophysics, photochemistry and dynamics of host–guest chemistry
- Using supramolecular effects for photocatalysis

1 Introduction

Nature's mastery of non-covalent interactions can be elegantly visualized in enzyme-catalyzed reactions.[1] One of the features that many of the enzymatic reactions often exhibit is their ability to sequester substrates in a reaction-ready configuration thereby lowering the activation energy for the chemical transformation(s) and expelling the product(s) due to unfavourable interactions within the confined environment of the enzymatic cavity. This perfect scenario fine-tuned during molecular evolution has inspired chemists to develop chemical systems that feature confinement and non-bonding interactions for catalysis.[2] To influence "molecular action" beyond the reactive substrates (called guests, G), it became necessary for chemists to build molecular architectures known as "supramolecules" (called hosts, H) that could potentially impact the outcome of a chemical transformation of interest (in particular photochemical transformations).[3] This review will highlight the role of supramolecules in promoting and controlling

light induced transformation(s) leading to supramolecular photocatalysis. For influencing photochemical and photophysical properties of guest molecules using confinement and non-bonding interactions that develop between the host and the guest three important features[4] have to be manipulated *viz.*, (a) structural rigidity that arises due to interactions between the supramolecular host(s) and the reactive guest(s); (b) the space and volume restrictions that influence the vibrational, rotational and translational motion of the guest(s) when interacting with the host(s); and (c) kinetic, thermodynamic and excited state properties of guest molecules within the supramolecular environment, resulting in efficient supramolecular photocatalysis.[4] Keeping these aspects in mind, various supramolecular assemblies based on organic and inorganic templates have been developed to enhance and control photochemical reactivity and selectivity and alter photophysical properties of guest molecules.[3,5] While detailed photophysical investigations are quite necessary for ascertaining the excited state properties of guest molecules, this review will focus on photochemical/catalytic reactivity of guest molecules under the influence of host. While acknowledging that there are several other well defined supramolecular hosts[5] like zeolites, micelles, dendrimers *etc.* that offer unique properties and impart excellent control on

Department of Chemistry and Biochemistry, North Dakota State University, Fargo, ND 58108-6050, USA. E-mail: sivaguru.jayaraman@ndsu.edu; Fax: +1-701-231-8831; Tel: +1-701-231-8923

4084 | *Chem. Soc. Rev.*, 2014, **43**, 4084–4101

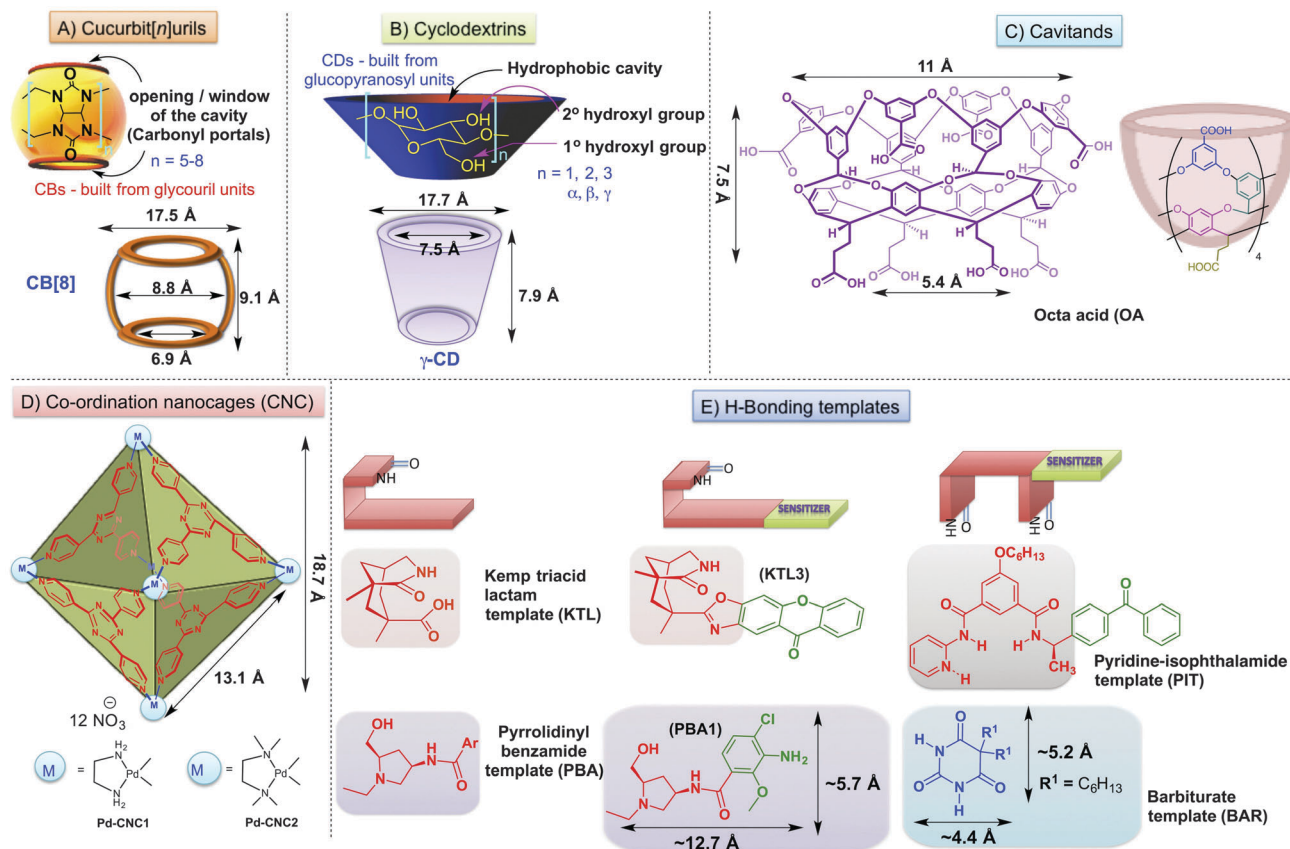This journal is © The Royal Society of Chemistry 2014

Fig. 1 Structural features of various supramolecular containers and supramolecular templates.

reactive substrates, for the purpose of this review, we will restrict ourselves to a few supramolecular hosts (Fig. 1 and Tables 1 and 2) *viz.* cucurbiturils,[4,6–8] cyclodextrins,[9] cavitands,[10] co-ordination nanocages,[11–13] H-bonding templates[14–21] and metallosupramolecular assemblies.[22–24] Readers are encouraged to refer to use of biomolecules and organized chiral templates for photochirogenesis reviewed by Inoue and co-workers[25] and template effects for controlling photoreactions in solution by Bassani and co-workers[26] and we will not highlight those aspects in this review.

Nandini Vallavoju

Ms Nandini Vallavoju obtained her Bachelor and Master degrees in chemistry from Osmania University, Andhra Pradesh, India in 2002 and 2004 respectively. She then worked in a pharmaceutical company (Dr. Reddy's Laboratories, Hyderabad, India) before moving to North Dakota State University for her doctoral studies in 2010. She is presently a 4th year graduate student performing her doctoral investigation under the mentorship of Prof. Sivaguru Jayaraman. Her research focus is on stereospecific and catalytic phototransformations.
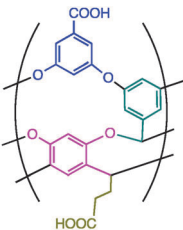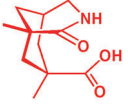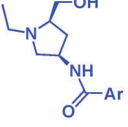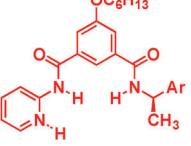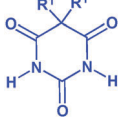

J. Sivaguru

Prof. Sivaguru (Siva) Jayaraman is an associate professor of Chemistry and Biochemistry at North Dakota State University, Fargo, ND. He is a recipient of the NSF-CAREER award (2008), Grammaticakis-Neumann Prize (2010) from the Swiss Chemical Society and Young-investigator awards from the Inter-American Photochemical Society (2011) and Sigma-Xi (2012). At NDSU, he has been honoured for both research (2010) and teaching (2011) and was also a recipient of the 2012 Peltier Award for Teaching Innovation. In 2013, he became the American editor for the Journal of Photochemistry and Photobiology-A: Chemistry, an Elsevier journal. His research interests include supramolecular photochemistry, asymmetric photochemistry, organo-photocatalysis and supramolecular photocatalysis.

This journal is © The Royal Society of Chemistry 2014

Chem. Soc. Rev., 2014, **43**, 4084–4101 | **4085**

Table 1 Structural parameters and physical properties of cyclodextrins (CDs) and cucurbiturils (CBs)

Entry	Parameters	Cyclodextrins (CDs)[a]			Cucurbit[n]urils (CBs)[b]		
		α-CD	β-CD	γ-CD	CB[6]	CB[7]	CB[8]
1	No of units	6	7	8	6	7	8
2	Molecular weight (anhydrous)	972	1135	1297	997	1163	1329
3	Water solubility (g L^{-1})	145	18.5	232	<0.18	<35.0	<0.15
4	Cavity height (Å)	7.9	7.9	7.9	9.1	9.1	9.1
5	Outside diameter (Å)	15.2	16.6	17.7	14.4	16.0	17.5
6	Portal diameter[a] (Å)	4.7	6.0	7.5	3.9	5.4	6.9
7	Inner cavity diameter[b] (Å)	5.3	6.5	8.5	5.8	7.3	8.8
8	Cavity volume (Å^3)	174	262	427	164	279	479
9	References	9	9	9	4, 7, 8	4, 7, 8	4, 7, 8

[a] Inner rim diameter of CDs. [b] Outer rim diameter of CDs.

Table 2 Structural parameters and physical properties of the co-ordination nanocage (CNC), octa acid (OA) cavitands and H-bonding templates

Entry	Supramolecular hosts	Structural unit	Dimension (Å)	References
1	Co-ordination nanocage (CNC)[a]	6 : 4 ratio of metal ions capped with ethylenediamine : 1,3,5-tris(4-pyridyl)triazine	∼18.7 (length) ∼13.1 (facial length)	11–13
2	Octa acid (OA)[b]		∼11 (top opening) ∼7.5 (height) ∼5.4 (bottom opening)	10, 27, 28
3	Kemp triacid lactam (KTL) template[c]		N/A	14–17
4	Pyrrolidinyl benzamide (PBA) template[d]		∼12.7 × ∼5.7 (PBA1)	18
5	Pyridine-isophthalamide (PIT) template[c]		N/A	19
6	Barbiturate (BAR) template[e]		∼4.4 × ∼5.2	20, 21

[a] Structural parameters from ref. 11–13. [b] Structural parameters from ref. 10, 27, 28. [c] NA = structural parameters not available. [d] Structural parameters from ref. 18. [e] The structural parameters from single crystal XRD CCDC number: 213543 and reproduced from ref. 20 with permission of The American Chemical Society.

2 Confinement and non-bonding interactions and their role in altering excited state properties

Light induced transformations involve reactive excited states that are short lived and can readily relax to their ground state through radiative and/or non-radiative transitions. This necessitates delicate control over molecular dynamics that influence excited state reactivity and selectivity as well as photophysical events. Over the last few decades, one of the successful strategies that has been developed to channel excited-state energy towards useful chemical transformations is by employing organized assemblies that pre-orient reactive molecule(s) in a configuration that is conducive for photoreaction(s). Dictating reactivity using supramolecular scaffolds enables chemists to efficiently

4086 | *Chem. Soc. Rev.*, 2014, **43**, 4084–4101

This journal is © The Royal Society of Chemistry 2014

carry out light-induced transformations that are generally inefficient in isotropic media (using solvent alone). As an added advantage, confinement of chromophores within supramolecular assemblies opens up avenues to alter/enhance their excited state properties. Other aspects that need to be considered are the physical properties (*e.g.* solubility) of the host that is employed as the supramolecular catalyst.

3 General considerations for supramolecular photocatalysis

Photocatalysis mediated by supramolecular assemblies typically requires host–guest interactions aided by non-covalent forces (*e.g.* hydrogen-bonding, van der Waals, Coulombic, and π–π interactions) leading to rate acceleration in the photoreaction of interest. For efficient supramolecular photocatalysis three important criteria need to be satisfied *viz.*, (1) the pre-orientation of reactant(s) in a configuration conducive for photochemical reaction(s) called "reaction-ready" configuration, (2) the quantum yield of photoreaction of interest (for both uni- and bi-molecular reactions) in isotropic media must be lower than the quantum yield of photoreaction within the supramolecular scaffold; and (3) dynamic exchange of reactant(s) and photoproduct(s) that enable sequestrating of reactant(s) and product release from the supramolecular scaffold leading to turnover and catalysis.

Understanding the above three fundamental criteria for supramolecular photocatalysis requires a clear comprehension of the thermodynamic and kinetic features involving host–guest interactions as well as the efficiency of photochemical transformations of the guest substrate sequestered by the supramolecular host. For the scope of this review we will restrict ourselves to photocatalysis of unimolecular and bimolecular transformations involving 1:1 (Fig. 2-top), 2:1 (Fig. 2-middle) and 1:2 (Fig. 2-bottom) host–guest complexes. One can extend our treatment of supramolecular photocatalysis to higher order host–guest complexes (*e.g.* 2:2 host–guest complex). Inspection of Fig. 2 shows that irrespective of the type of host–guest complex (1:1, 2:1 or 1:2), a clear understanding of supramolecular host–guest interactions reflected by the thermodynamic binding constant (K_a) for the reactive guest(s) and thermodynamic dissociation constant (K_d) for the photoproduct(s) is necessary.[29] For catalytic turnover, the binding affinity of the reactive guest(s) substrate should be greater or at the very least comparable to the binding affinity of the photoproduct(s) with the supramolecular host to prevent product inhibition during the catalytic processes. To appreciate catalytic turnover, it is critical to ascertain the kinetics of the individual microscopic steps (both forward and reverse rate constants). Finally, the efficiency of the photochemical transformation mediated by the supramolecular host is quantified through reaction velocity measurements or quantum yield studies. Experimentally, the thermodynamic parameters of the host–guest complex can be determined by fluorescence titrations or by using isothermal calorimetric titrations (ITC) and the kinetics of the complexation process can be ascertained by stopped flow measurements. As a self-check mechanism, the forward and reverse rate constants should reflect the
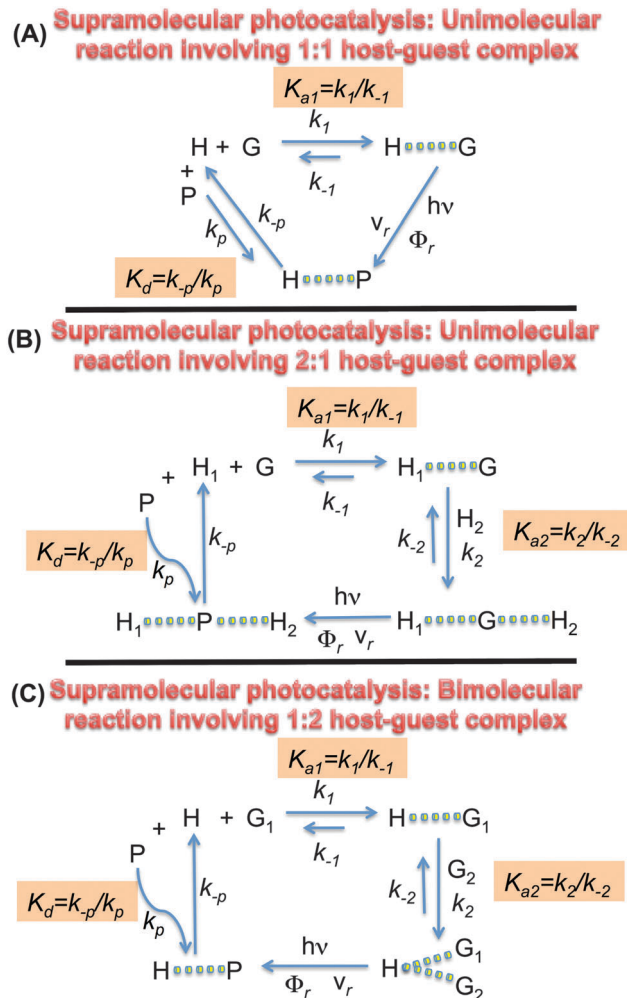

Fig. 2 Paradigm for supramolecular photocatalysis and host–guest chemistry. H and G represent the host and guest respectively. K_a represents the thermodynamic binding affinity of the guest with the host for the individual host–guest complex formation steps. K_d is the dissociation constant for the product from the supramolecular host. k_1, k_{-1}, k_2 and k_{-2} are the forward and reverse rate constants for individual microscopic steps leading to the host–guest formation. k_p and k_{-p} are the rate constants for product association and dissociation with the supramolecular host. Φ_r and V_r represent the quantum yield and reaction velocity of photoreaction mediated by the supramolecular host.

thermodynamic binding constants for individual microscopic steps involved in the complexation. The quantum yield of the photoreaction can be determined by actinometry measurements and the reaction velocity can be measured by various analytical techniques (*e.g.* UV-Vis). Thus the use of multiple analytical techniques not only aids in the understanding of host–guest interactions but also provides a path for evaluating the efficiency of the photochemical transformation of interest.
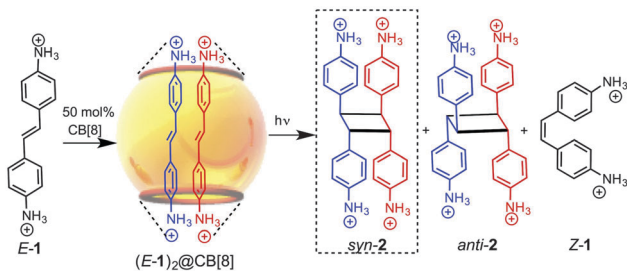
4 Examples of supramolecular photocatalysis

4.1. Cucurbit[*n*]urils

Cucurbit[*n*]urils (CBs) represent a family of macrocyclic compounds originally synthesized by Behrend and co-workers[6] in

This journal is © The Royal Society of Chemistry 2014

*Chem. Soc. Rev.*, 2014, **43**, 4084–4101 | **4087**

1905 from an acid-catalyzed condensation reaction of form-aldehyde with six glycouril units (cucurbit[6]uril; Table 1). The name cucurbituril was coined by Mock and co-workers[30] as these supramolecules resembles pumpkins in shape whose botanical name is *cucurbitacae*. In the early 2000s Kim[31] and Day[32] independently reported the synthesis of higher homologues of cucurbituril with seven glycouril units known as cucurbit[7]uril (CB[7]) and eight glycouril units known as cucurbit[8]uril, CB[8]. Recent developments[7,8,33] have enabled the synthesis of func-tionalized cucurbiturils. For the scope of this tutorial we will concentrate on the ability of CB[8] and CB[7] to catalyse photo-chemical reactions as exemplars for understanding supra-molecular catalysis.[4]

Employing sub-stoichiometric amounts of CBs to enhance chemical reactivity was first reported by Kim and co-workers.[34] The stereoselective [2+2]-photodimerization of (E)-diaminostilbene **1** (Scheme 1) was evaluated by employing 50 mol% of CB[8]. Selective formation of the corresponding *syn*-**2** photodimer was observed with a *syn*:*anti* ratio of 95:5. In addition, the confin-ing environment of CB[8] prevented the facile *E/Z* isomerization of stilbene that is observed in solution. The high efficiency for the formation of *syn*-**2** was attributed to the formation of a stable 1:2 (E-**1**)$_2$@CB[8] host–guest complex. The binding con-stant of this ternary complex in formic acid–water (2:3 ratio) was reported to be 3.8×10^4 M^{-2} by isothermal titration calorimetry. In the above example, while the cationic nature of the reactive guest enabled efficient formation of the host–guest complex, the photoproduct release was not very facile and this necessitated the use of 50 mol% of the supramolecular scaffold. Nevertheless, the study successfully demonstrated the utility of CB[8] as a nano-container in which two cationic guest molecules were oriented in close proximity that could facilitate photoreactions with high control over regiochemistry and stereoselectivity.

Building on this precedent of effective encapsulation of cationic guest molecules by cucurbiturils, Ramamurthy and co-workers employed CB[8] for photodimerization of *trans*-1,2-bis(*n*-pyridyl)ethylene **3a–c** as well as *trans*-stilbazole **3d** in aqueous solution.[35,36] The host–guest complexation between E-**3a** and CB[8] was evaluated by NMR titrations. The binding constants were found to be 1.03×10^3 M^{-1} (K_{a1}) and 8.6×10^5 M^{-1} (K_{a2}) for the formation of 1:1 and 1:2 host–guest com-plexes respectively.[36] They observed efficient photodimerization in
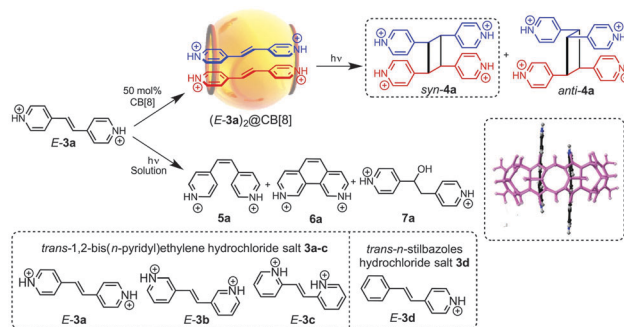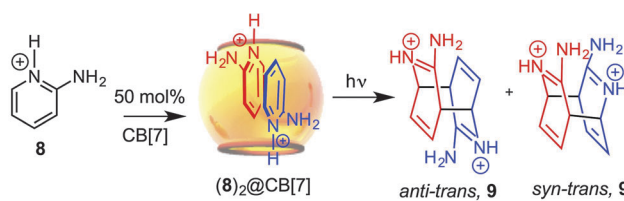

Scheme 2 CB[8] mediated photodimerization of *trans*-1,2-bis(*n*-pyridyl)-ethylene and stilbazole in aqueous media. Single-crystal XRD of the CB[8]-(E)-**3a** 1:2 host–guest complex. XRD structure rendered from cif file CCDC No. 276220 and reproduced from ref. 35 with permission of The Royal Society of Chemistry.

the presence of 50 mol% of CB[8] yielding *syn*-dimer **4**. Irradiation in the absence of CB[8] gave the isomerized photoproduct **5**, the intramolecular cyclization product **6** as well as the hydration product **7** (Scheme 2).

While CB[8] can be used to efficiently sequester two large cationic organic molecules to influence photochemical reactivity, CB[7] may also be employed for appropriately designed small guest molecules that can be accommodated within its hydro-phobic cavity. The contrasting features between the two cucur-biturils (Table 1) are their differences in volume (279 Å^3 in CB[7] *vs.* 479 Å^3 in CB[8]) and solubility in water (CB[7] is more soluble than CB[8]). [4+4]-Photodimerization of 2-aminopyridine hydro-chloride **8** in the presence of CB[7] was reported by Macartney and co-workers (Scheme 3).[37] The [4+4]-photodimerization of **8** was observed to be very selective in the presence of CB[7] in aqueous solution leading exclusively to the formation of the *anti*-*trans*-dimer **9**. However, in the absence of CB[7], both the *anti*-*trans* **9** and *syn*-*trans* **9** photodimers were observed in a ratio of 4:1. The authors reasoned that addition of the CB[7] stabilized the photoproduct **9**, thus preventing the rearomatization of **9** to the 2-aminopyridine monomer at room temperature.

The ability of cucurbiturils to confine molecules allow for an increased chance of collision between the reactive partners leading to rate acceleration/catalysis. One of the common features in the studies detailed above is the use of cationic substrates, as the ion–dipole and hydrogen bonding interactions between cationic groups of guest and portal carbonyl groups of the host, as well as the developing hydrophobic interaction between host and guest favoured a thermodynamically stable host–guest complex.


Scheme 1 Stereoselective [2+2]-photodimerization of (E)-diaminostilbene mediated by CB[8] in solution.

Scheme 3 CB[7] promoted [2+2]-photodimerization of aminopyridines in solution.

This presents a bottleneck in which the photoproduct that is formed within the supramolecular cavity is not efficiently expelled to enable catalysis and turnover. This product inhibition has its origin in the strong binding of the guest (in this case photoproduct) that is aided by the same ion–dipole and hydrophobic interactions that facilitated the host–guest formation between the reactive substrate and the supramolecular host. In addition, in spite of being sub-stoichiometric, employing 50 mol% of CB[8] does not fully address the issue of low solubility of CB[8] (Table 1) compared to the corresponding cyclodextrin analogue (γ-CD). This necessitated a strategy for sequestering neutral molecules instead of cationic guests within the supramolecular container and controlling their photoreactivity with less than 50 mol% of the host leading to efficient product formation followed by the expulsion of the photoproduct (that will be neutral) leading to turnover and catalysis.[4]

In this regard, we reported photodimerization of neutral molecules (coumarin derivatives) in the presence of catalytic amounts (10 mol%) of CB[8] in aqueous media.[4,38–40] We employed 6-methylcoumarin (**10**; Scheme 4) as the model system, as its photochemical reactivity in solution and in organized assemblies is well established in the literature.[38,40] In the absence of CB[8] the photodimerization of **10** was inefficient (<10% conversion; 60 min irradiation) in water leading to the formation of both *syn-* and *anti-* adducts. On the other hand, the reaction (for the same 60 min irradiation) was found to be clean and efficient in the presence of CB[8] in water leading to the exclusive formation of *syn*-dimers with a *syn*-HH **11**/*syn*-HT **13** ratio of about 70:30. As we were successful in crystallizing the 1:2 host–guest complex (Fig. 3A), it gave insights into the role of confinement in influencing the excited state chemical reactivity of coumarin derivatives.

Inspection of the single-crystal XRD structure revealed that the 1:2 CB[8]–**10** host–guest complex had a head-to-tail (HT) orientation (Fig. 3A). If the same orientation were to be preferred during photochemical reaction, one would predict the HT photodimers (*syn*-HT **13** and *anti*-HT **14**; Scheme 4) as major products. The preferential formation of *syn* photoproducts in the presence of CB[8] was likely due to a combination of effects *viz.*, the different orientation of the guest molecules within CB[8] in solution compared to the crystalline environment
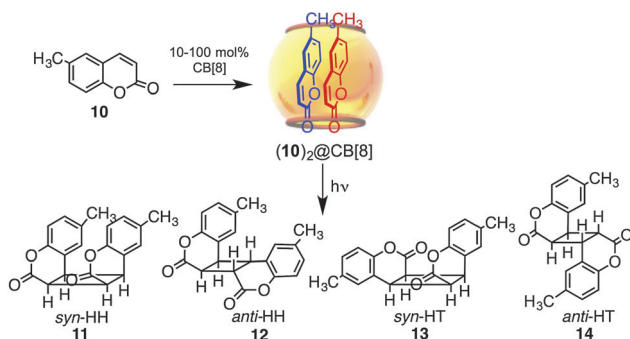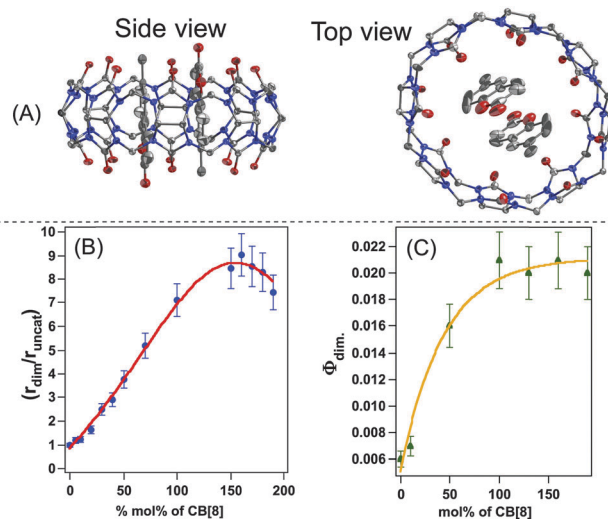

Fig. 3 (A) Single-crystal XRD of the (**10**)$_2$@CB[8] complex. (B) Photodimerization rate increases upon varying the mol% of CB[8]. r_{uncat} is the rate of photodimerization in the absence of CB[8] in water and r_{dim} is the rate of photodimerization in the presence of CB[8]. (C) Photodimerization quantum yield, Φ_{dim} with varying the mol% of CB[8]. The single crystal XRD structure rendered from the CCDC 814052 cif file and adapted from ref. 40 with permission from The Royal Society of Chemistry. Figures B and C were reproduced from ref. 39 with permission from Canadian Journal of Chemistry.

and/or the HH orientation of the 1:2 host–guest complex being more reactive in solution in the presence of CB[8] than the HT orientation leading to a *syn*-HH **11**/*syn*-HT **13** ratio of about 70:30. It was also found that the reaction could be efficiently carried out with sunlight in water leading to similar selectivity to Hg lamp irradiation.[38,40]

One of the key aspects that was observed during the photodimerization of **10** was the exclusive formation of *syn* dimers within the CB[8], while *anti* dimers are observed only in water and in isotropic media. This presented a clear track to gauge the dimerization efficiency inside the CB[8] cavity. This difference in the product stereochemistry allowed us to pin-point the location of photodimerization of **10** when a sub-stoichiometric amount of CB[8] was employed. For example, as *anti* dimers were not observed upon employing 10 mol% (or higher) of CB[8], the photodimerization likely occurred within the CB[8] cavity.

To quantify the supramolecular photocatalytic efficiency, photochemical and photophysical parameters were evaluated (Fig. 3 and 4). The photodimerization kinetics was followed at various mol% of CB[8] and the reaction rate (r_{dim}) was found to increase upon increasing the mol% of CB[8]. The maximum rate of photodimerization in the presence of CB[8] was ∼9.0 times (Fig. 3B) faster than the uncatalyzed reaction (r_{dim}/r_{uncat} = 9.0). The dimerization efficiency was lowered upon further increase of CB[8] concentration. This was attributed to the formation of aggregates of CB[8] at high concentration as well as the formation of 1:1 host–guest complex that decreased the amount of 1:2 host–guest complex in solution that is responsible for the enhanced rate of photodimerization. The quantum
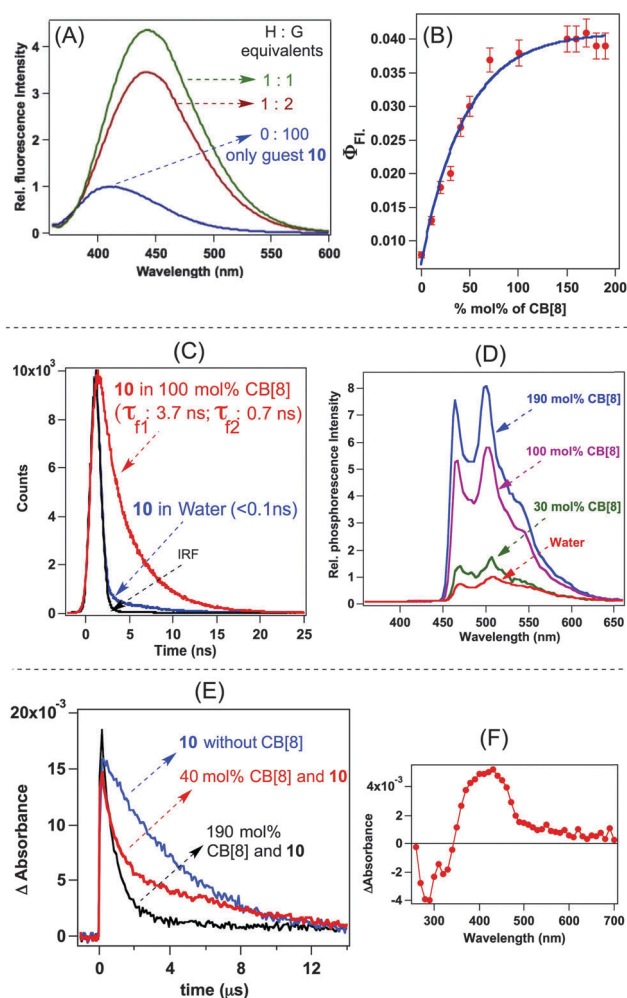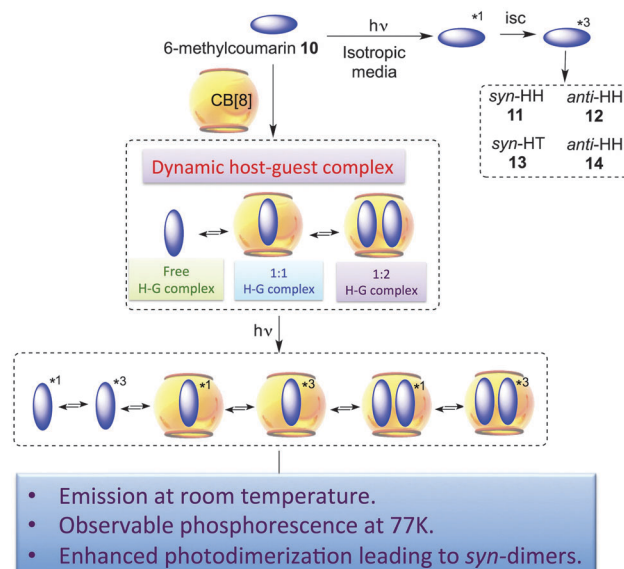

Scheme 4 Photodimerization of 6-methylcoumarin catalyzed by CB[8].

Fig. 4 (A) Steady-state emission of **10** at 298 K (λ_{ex} = 320 nm) with various equivalents of CB[8]. (B) Change in fluorescence quantum yield, Φ_{Fl} with varying the mol% of CB[8]. (C) Fluorescence decay of **10** at 298 K (λ_{ex} = 340 nm; λ_{em} = 411 nm for decay in water and λ_{em} = 443 nm for 100 mol% of CB[8]); IRF = instrument response function. (D) Phosphorescence of **10** at 77 K in water recorded from a 30 to 60 ms time window with various mol% of CB[8] (relative to the concentration of **10**); λ_{ex} = 345 nm. (E) Transient absorption decay traces recorded at 420 nm of ^{3}(**10**)* in the absence and presence of different amounts of CB[8]. (F) Transient absorption spectrum of the CB[8]–**10** host–guest complex (25 mM CB[8] and 50 mM **10**). Figures B, C and D were reproduced from ref. 39 with permission from Canadian Journal of Chemistry. Figures A, E and F were reproduced from ref. 40 with permission from The Royal Society of Chemistry.

the guest. In other words, the system was quite dynamic leading to exchange of guest molecule(s) with the host that manifested itself during supramolecular photocatalysis.

Fluorescence studies on **10** in the absence of CB[8] showed a structureless emission (Fig. 4A) centered at around 411 nm. Complexation of **10** within CB[8] resulted in an increase in the emission intensity with a noticeable red shift with the emission maximum centered at around 443 nm (Fig. 4A). In addition, the fluorescence lifetime of **10** was found to increase in the presence of CB[8]. The fluorescent decay analysis showed that uncomplexed **10** had a fluorescent lifetime (τ_f) of <0.1 ns (Fig. 4C). In the presence of CB[8], in addition to the uncomplexed **10**, a 1:1 CB[8]–**10** host–guest complex with τ_f = 3.7 ns and a 1:2 CB[8]–**10** host–guest complex with τ_f = 0.7 ns were observed (Fig. 4C). Phosphorescence at 77 K (Fig. 4D) in water was observed in the presence of CB[8] that showed the involvement of a triplet excited state of **10**. Thus in addition to a dynamic host–guest system, where uncomplexed **10** co-existed with 1:1 and 1:2 CB[8]–**10** host–guest complexes in water, upon light excitation the corresponding singlet and triplet excited states of the dynamic mixture (uncomplexed and complexed guests) were generated in solution (Scheme 5). The confinement of **10** within the hydrophobic CB[8] cavity was reasoned to be responsible for the enhanced fluorescence emission intensity and longer lifetimes. Similarly, the confinement of **10** within CB[8] was reasoned to be responsible for the observed phosphorescence at 77 K. In solution, the excited **10** formed a mixture of photoproducts **11–14** as there was no control over the excited state reactivity/dynamics. On the other hand, the confined environment of CBs not only influenced the excited state lifetimes, but also channeled the excited state energy towards photochemical reactivity leading to photoproduct selectivity.

yield of photodimerization (Φ_{dim}) was found to increase with increasing mol% of CB[8]. From inspection of Fig. 3C it is clear that the Φ_{dim} levels off beyond 70 mol% of CB[8]. There was no noticeable change in Φ_{dim} upon increasing the mole equivalents of CB[8] beyond 100 mol%. This indicated that photoreaction beyond 70 mol% of CB[8] occurred at the same efficiency i.e., the syn-photodimer formed per unit of time to the number of photons absorbed was similar beyond 70 mol% of CB[8]. On the other hand, the rate of photodimerization (r_{dim}) depended on the relative population of the 1:2 H–G complex, the 1:1 H–G complex, and uncomplexed **10**, which in turn were dependent on the relative amounts of the host and

Scheme 5 Interplay of supramolecular complexation dynamics and its effects on excited state photophysics and photochemistry. Reproduced from ref. 39 with permission from Canadian Journal of Chemistry.

Table 3 Triplet lifetimes (τ) and pre-exponential factors (A) of transient absorption decays of $^3(\mathbf{10})^*$ at 420 nm with various mol% of CB[8][a]

Entry	mol% CB	τ_1 (μs)	A_1	τ_2 (μs)	A_2
1	0	4.6	25	—	—
2	10	5.4	14	0.75	2.6
3	70	12	2.5	0.75	20
4	100	—	—	0.74	36
5	190	—	—	0.75	37

[a] Laser pulse (308 nm, pulse width 15 ns). The decays were fitted to: Δabsorbance $(t) = A_1 \exp(-t/\tau_1) + A_2 \exp(-t/\tau_2)$. Data reproduced from ref. 40 with permission from The Royal Society of Chemistry.

The photodimerization of **10** mediated by CB[8] was efficient under nitrogen, air or oxygen saturated conditions with no noticeable difference in the reaction conversion. This led to the suggestion of two distinct possibilities on how the excited states of **10** were influenced by complexation within CB[8]. In the first scenario, a singlet excited state of **10** was conjectured to be involved in the photodimerization pathway mediated by CB[8]. In the second scenario, a triplet excited state of **10** mediated the photodimerization upon encapsulation within CB[8]. This triplet excited state of **10** encapsulated within CB[8] was shielded from external quencher(s) namely, ground state molecular oxygen for a longer time compared with uncomplexed **10** outside the cavity leading to enhanced photoreactivity. As phosphorescence was measured at 77 K and the photochemical reactivity was carried out under ambient conditions, laser flash photolysis studies were performed under similar reaction conditions (Table 3) to understand the triplet state dynamics involved during supramolecular photocatalysis.

The transient absorption spectrum (Fig. 4F) of deoxygenated aqueous solution of **10** was generated using 308 nm laser excitation (Table 3) and the triplet absorption decay traces were recorded at different concentrations of CB[8] (Fig. 4E and Table 3). In the absence of CB[8], the triplet-excited state of **10** was found to decay mono-exponentially with a lifetime (τ_1) of 4.6 μs (Table 3; entry 1). In the presence of 100 mol% of CB[8] or higher, a mono-exponential triplet decay with a lifetime (τ_2) of $\sim$0.75 μs was observed that was assigned as the triplet excited state of **10** encapsulated within CB[8]. Between 10 mol% and 100 mol% of CB[8] a bi-exponential triplet kinetic decay was observed with a short component ($\tau_2 \sim 0.75$ μs) and a long component with lifetimes (τ_1) varying between 5.4 and 12 μs (Table 3, entries 2 and 3). The contribution of the short component (τ_2) increased with increasing concentration of CB[8] and was exposed by the increase of the pre-exponential factor (Table 3). The varying lifetime (τ_1) was rationalized based on efficient self-quenching of triplet excited **10** with a rate constant of 4.1×10^9 M^{-1} s^{-1}. Due to supramolecular encapsulation of **10** within CB[8], the fraction of uncomplexed **10** decreased in aqueous solution with increasing CB[8] concentrations that was reflected in the decrease in A_1 values (Table 3). This decrease in the effective concentration of uncomplexed **10** upon addition of CB[8] resulted in a decreased self-quenching rate of triplet excited **10**. This decrease in the rate of self-quenching resulted in the increase in the transient lifetime as

displayed by τ_1 values upon increasing concentration of CB[8]. The photoexcited 1 : 2 CB[8]–**10** HG complex was short lived and was not detected during the transient decay kinetic study due to enhanced deactivation of the excited state by the proximity effect. In addition, the triplet excited **10** encapsulated within CB[8] was not effectively quenched by molecular oxygen, while triplet excited **10** that was uncomplexed in aqueous solution was quenched effectively with a high rate constant of 2×10^9 M^{-1} s^{-1}. This implied that the triplet-excited state of **10** upon encapsulation with the CB[8] cavity was protected from quenching by molecular oxygen. This protective encapsulation of the triplet excited state was rationalized to be responsible for the similar conversions observed under nitrogen and oxygen saturated atmospheres.

The enzyme-mimetic nature of supramolecular photocatalysis was evident from saturation kinetics that gave a turnover frequency of 3.4 min^{-1} with sigmoidal dependence on coumarin concentration (with constant CB[8] concentration) that implied that the overall catalytic process was cooperative in nature (Fig. 5A). The origin of the sigmoidal dependence was deciphered by a Hill plot that gave a Hill constant of 1.8 implying a positive allosteric effect in the catalytic process. Based on the above detailed photochemical, photophysical and kinetics studies, a representative catalytic cycle involving CB[8] mediating the photodimerization of **10** was proposed (Fig. 5B), in which the formation of a 1 : 1 CB[8]–**10** host–guest complex
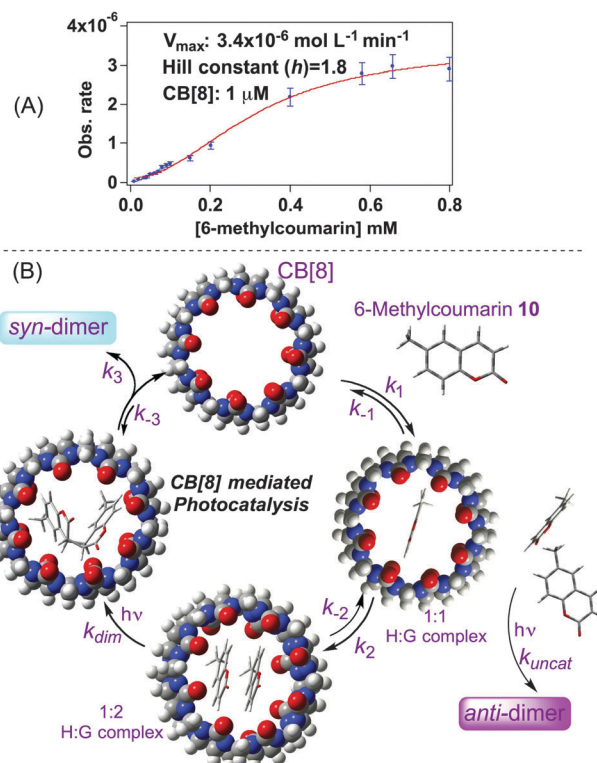

Fig. 5 (A) Saturation kinetics of CB[8] mediated photocatalysis of **10**. (B) Supramolecular photocatalysis of 6-methylcoumarin **10** mediated by CB[8]. Figures A and B reproduced from ref. 38 with permission from The Royal Society of Chemistry.

This journal is © The Royal Society of Chemistry 2014

Chem. Soc. Rev., 2014, 43, 4084–4101 | 4091

was followed by the formation of a 1 : 2 CB[8]–**10** host–guest complex. To understand the catalytic process involved in the photodimerization involving CB[8], thermodynamic binding constant measurements were done using fluorescence titrations and the kinetic aspects of host–guest complexation were determined by stopped-flow spectrometry. Thermodynamic binding constants for the formation of 1 : 1 and 1 : 2 CB[8]–**10** host–guest complexes were found to be K_{a1}: 1.3×10^4 M^{-1} and K_{a2}: 2×10^6 M^{-1} respectively.[39]

Control studies showed that there was no product inhibition during the photocatalysis mediated by CB[8].[41] Based on the difference in the fluorescence intensity observed for **10** with various mol% of CB[8], stopped-flow kinetic measurements were performed to ascertain the host–guest complexation rate constants. Stopped-flow data indicated that the formation of the 1 : 1 CB[8]–**10** host–guest complex was kinetically fast and formation of the 1 : 2 CB[8]–**10** host–guest complex was slow and it was likely to serve as the rate limiting step during the CB[8] supramolecular photocatalytic process. The reason conjectured for the slow second step *i.e.*, the formation of the 1 : 2 HG complex, in spite of being thermodynamically favorable was due to the longer time required for the first coumarin guest molecule to alter the shape of the CB[8] cavity to accommodate the second coumarin guest molecule that was reflected in the allosteric response observed in the saturation kinetics measurements. This guest induced shape change that mediated the supramolecular catalysis by CB[8] was reminiscent of enzyme catalysis. The catalytic cycle involving CB[8] was a prototype of the paradigm we generalized in Fig. 2C with the sequential formation of a 1 : 2 host–guest complex that reacts efficiently upon excitation with light. While the working aspects of these systems will not be much different one can envision a catalytic cycle involving other supramolecular assemblies (*vide infra*). Keeping in mind the space limitation and the scope of this tutorial review, we will just highlight the use of different supramolecular assemblies to enhance reactivity and selectivity in photoreactions. One can perform detailed analysis (as we did for the CB[8]–coumarin system) to understand the intricacies involved in the supramolecular catalysis involving various organized assemblies to comprehend their influence in light initiated reactions.

4.2. Cyclodextrins

Cyclodextrins (CDs) are cyclic oligosaccharides that consist of six to eight D-glucopyranose units, which are linked by 1,4-glycosidic bonds (Fig. 1).[9] Structurally cyclodextrins resemble a cone or a truncated funnel. CDs have two different portals, a narrow portal that consists of primary hydroxyl groups and a wider portal that consists of secondary hydroxyl groups. The central cavity consists of D-glucopyranoside units made of carbon atoms with an ether linkage, which gives CDs their hydrophobic character. It is this cavity that gives CDs their unique complexation ability in aqueous solution. Some of the potential applications of CDs include their critical role as catalysts in biomimetic reactions, organic reactions and drug delivery systems.[9] While there are numerous reports by
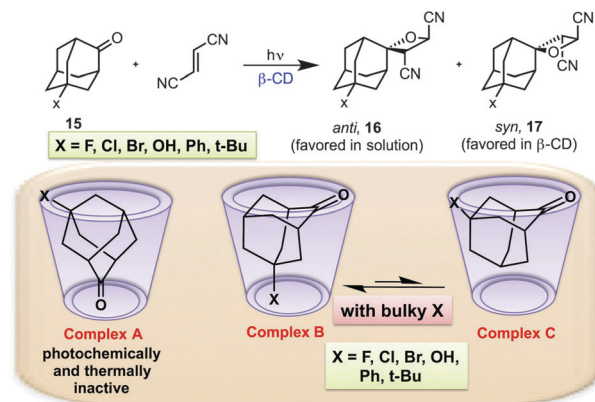

**Scheme 6** Paternó–Büchi reaction of adamantan-2-ones **15** with fumaronitrile mediated of β-cyclodextrin.

different groups on controlling photochemical reactivity by employing CDs as reaction flasks, we will highlight only a few selected examples of cyclodextrin and its derivatives mediating light induced transformations.

Turro and co-workers[42] have reported Paternó–Büchi reaction of adamantan-2-ones **15** with fumaronitrile (Scheme 6) in the presence of β-cyclodextrins (β-CDs). Irradiation of 5-substituted adamantan-2-ones **15** with fumaronitrile in aqueous media containing β-CD resulted in oxetanes favoring *syn* isomer **17**, while the *anti* isomer **16** was preferred in isotropic media and no significant change was observed in the presence of α- and γ-CD. The facial selectivity within β-CDs was rationalized based on the interaction of the carbonyl group with the β-CD host (represented by host–guest complexes A–C in Scheme 6).[42]

Inoue and co-workers have reported [4+4] photocyclodimerization of 2-anthracenecarboxylate **18** by employing γ-cyclodextrin (γ-CD) as a chiral template (Scheme 7).[43] The large cavity volume of γ-CD enabled two aromatic molecules to be accommodated within its cavity making them very attractive as templates for bimolecular photochemical transformation. A very stable 1 : 2 inclusion complex with γ-cyclodextrin (γ-CDs) was observed with thermodynamic binding constants of K_{a1} = 161 M^{-1} and K_{a2} = 3.85×10^4 M^{-1} at 25 °C. Photoinduced cyclodimerization of **18** in aqueous solution at 25 °C in the presence of γ-CD gave all the four photodimers. The *syn-head-to-tail*
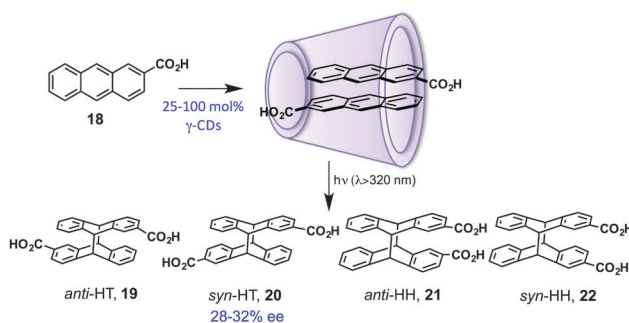
Scheme 7 [4+4]-Photocyclodimerization of 2-anthracenecarboxylate **18** catalysed by γ-cyclodextrin (γ-CD).
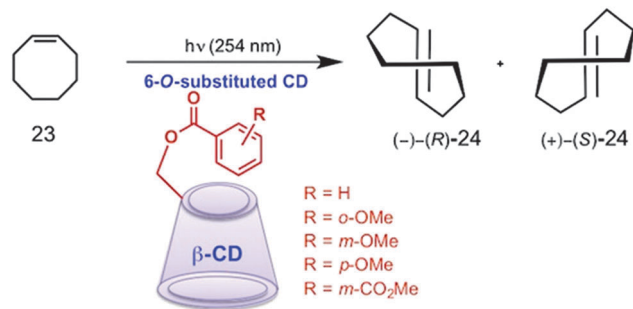
Scheme 8 Enantiodifferentiating photoisomerization of (Z)-cyclooctene to chiral (E)-cyclooctene induced and sensitized by 6-O-substituted-β-cyclodextrins.

dimer **20** was formed with an enantiomeric excess (ee) value of 32% at 25 °C. The observed selectivity was rationalized based on the structural isomers of the 1:2 γ-CD–**18** complex that was preferred in solution. These structural isomers of the 1:2 γ-CD–**18** complex were dependent on the different longitudinal orientation of the guest molecules (orientational isomers) within the γ-CD cavity. The population of the orientational isomers of the 1:2 γ-CD–**18** complex in the ground state before photoreaction manifested themselves in the stereoisomeric features/ratios of the photodimerization products. This was postulated because altering the orientation of **18** encapsulated within γ-CD was not feasible within its short excited singlet state lifetime. The origin of enantioselectivity in the chiral cyclodimer(s) stemmed from the difference in the stability/activation energy of the diastereomeric pair of orientational isomers of the 1:2 γ-CD–**18** complex. The ee in the chiral cyclodimer **20** was 28–32% at 25 °C and was dependent on the loading level of the cyclodextrin (25–100 mol%). The ee value increased to 41% in the cyclodimer **20** at 0 °C that highlighted the role of temperature in the enantio-differentiating process within the supramolecular container.
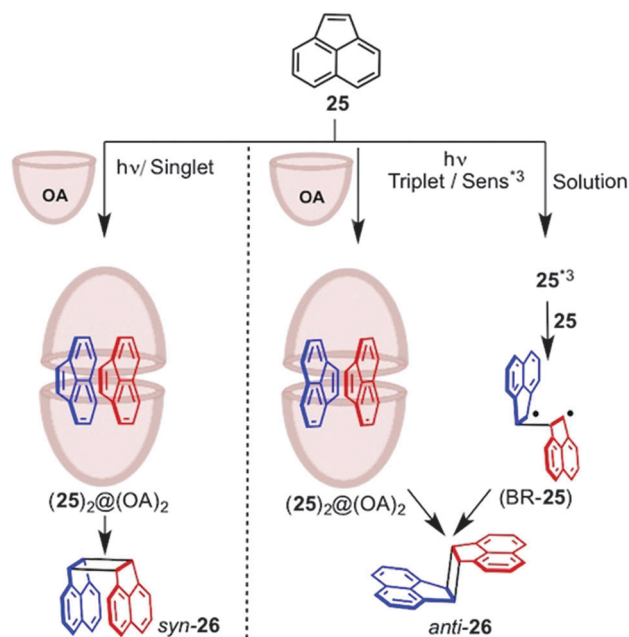
Inoue and co-workers[44] reported enantiodifferentiating photoisomerization of (Z)-cyclooctene **23** to chiral (E)-cyclooctene **24** mediated by 6-O-substituted cyclodextrins functionalized with an aromatic carboxylate as a sensitizer (Scheme 8). A series of α-, β-, and γ-CDs were prepared to fine-tune the space/bulkiness of the sensitizer (benzoates, isomeric phthalates and tethered benzamides). They observed that the photostationary state (**24**/**23** ratio) obtained upon sensitization of **23** with 6-O-substituted cyclodextrins in 1:1 water–methanol was between 0.4–0.8, while the photostationary state was ∼0.25 for sensitizations by conventional alkyl/alkoxy benzoates (that lacked the CD cavity) in hydrocarbon solvents. Low ee values were observed in the E-isomer **24** with α-CDs (3% ee) and γ-CDs (5% ee), which were rationalized due to the size-mismatch of the CD cavity. On the other hand, β-CD derivatives gave high ee values (ee values of up to 24%) in **24** due to cavity size matching with the reactive substrate.
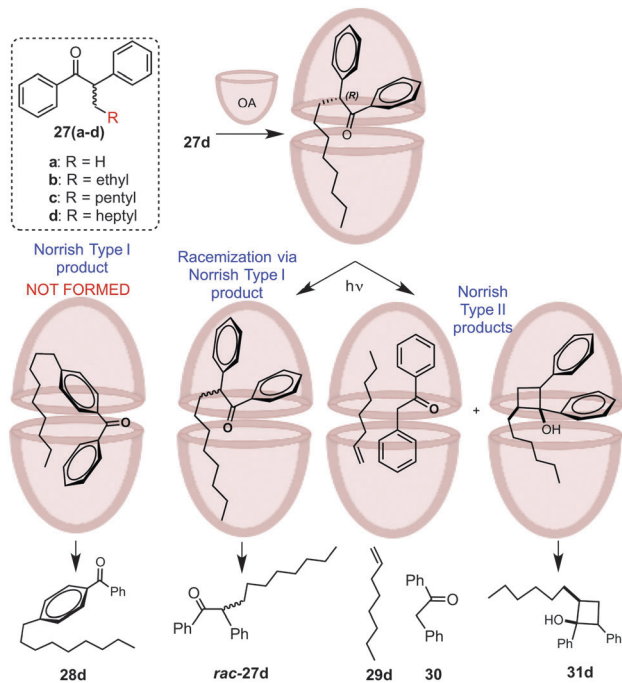
4.3. Cavitands

Cavitands are hosts based on various aromatic functionalities that have been synthesized over the years to modulate their supramolecular characteristics.[10,27,28] We will restrict our

discussions to a deep cavity cavitand known as octa acid (OA) that was synthesized by Gibb and co-workers[10] and has been successfully employed to control photochemical transformations and photophysical events.[27,28,45] While the shape of an octa acid cavitand is very reminiscent of cyclodextrins (Fig. 1), OA is a deep cavity cavitand due to two stacked aromatic units with a total of eight carboxylic acid groups. This makes it water soluble with a well-defined hydrophobic pocket. OA deep cavity features a larger portal of ∼11 Å and a shorter portal of ∼5.4 Å. The depth of the cavity is ∼7.5 Å (Fig. 1). The organic guest molecules enter the deep cavity through the larger OA portal. Depending on the type of guest(s), 1:1 and/or 2:2 host guest complexes were observed with OAs and were investigated for controlling light initiated processes. We will detail a couple of reactions that make use of OA to control photochemical reactivity. While not catalytic, OA in principle could be employed for supramolecular photocatalysis. Additionally, Ramamurthy and co-workers have also established that the OA capsules are not dormant spectators during photochemical reactions but are active in enabling energy and electron transfer reactions with appropriately designed guest molecules.[45] This provides new opportunities to develop supramolecular systems that can communicate with one another leading to molecular recognition and photocatalysis making them fertile grounds for future development.[45]

Pioneering work from Ramamurthy and co-workers established the use of OA for controlling the excited state photochemistry and photophysics of encapsulated organic molecules.[27] We will just highlight a couple of photochemical processes (Schemes 9 and 10) that were controlled within the confined environment of OA. A 2:2 host–guest complex (25_2@OA_2) was observed between OA and acenaphthylene **25** in water

Scheme 9 Photodimerization of acenaphthylene **25** in the presence of octa acid (OA).

This journal is © The Royal Society of Chemistry 2014

Chem. Soc. Rev., 2014, **43**, 4084–4101 | **4093**

Scheme 10 Photolysis of α-alkyl deoxybenzoins (α-ADBs) within a water-soluble octa acid.

(pH ~ 9, borate buffer).[27] Direct irradiation of the 2:2 complex resulted in the exclusive formation of *syn*-26 due to the preferential pre-orientation of the aromatic guests in a configuration conducive for the formation of *syn*-26 (Scheme 9). Triplet sensitized irradiation was performed using Eosin that resulted in *syn*-26 and the *anti*-26 (*syn*-26 : *anti*-26 = 3 : 2). The contrasting selectivities observed from singlet and triplet reactivity of 25 in the presence of OA was rationalized based on the excited state lifetimes and the dynamics of host–guest complexation. It was postulated that the short singlet lifetime of 25 (0.35 ns) did not allow the pre-oriented configuration to change its orientation/structural geometric features that led to the *syn*-26 photoproduct. For sensitized dimerization the long lifetime (6 ms) of the triplet excited state of 25 allowed the substrate excimers to escape from the OA capsule, which led to the reorientation of their geometry resulting in the formation of the *anti*-26 photoproduct (Scheme 9). The study highlighted the use of confining cavitands to pre-orient the substrates in a reaction ready configuration leading to a specific product as well as restrict molecular movements of substrates within the OA cavity that was dependent on the excited state lifetimes of the reactive substrates. In addition, the study also highlighted how dynamic aspects of host–guest complexation related to the excited state lifetimes of the reactants and how their kinetics influenced the photoproduct selectivity.

Ramamurthy and co-workers also reported the Norrish Type I and Type II reactions of optically pure α-alkyl deoxybenzoins 27 within the OA nanocapsule (Scheme 10).[28] A 2 : 1 host–guest complex was observed with octa acid (27@OA₂), a scenario depicted in Fig. 2B. Different alkyl substituted deoxybenzoins 27a–d were investigated to elucidate the role of alkyl substituents.

Photochemical reactivity was evaluated by irradiating the 27@OA₂ complex in borate buffer (Scheme 10) and was compared to the photochemical reactivity in isotropic media (benzene). Photoreaction of 27b–d in isotropic media (benzene) yielded both Norrish Type I and Type II products except for substrate 27a that gave Type I photoproducts. However, in the presence of OAs in borate buffer solution Type I rearrangement products were observed with 27a–b, whilst Type II products were observed with 27c–d. As optically pure isomers were employed, the optical activity after irradiation was dependent on the length of the alkyl chain in 27. It was postulated that the OA capsules were able to enforce conformation control that influenced the product distribution and the length of the alkyl chain determined the free space available within the confined environment. With shorter alkyl substituents in 27, the racemization product was attributed to free tumbling of the α-alkyl benzyl radical or sliding of the benzoyl radical within the OA cavity. With long alkyl chain substituents in 27, it was postulated that the reactants adopted a conformation that was suitable for Type II reaction within the OA cavity.
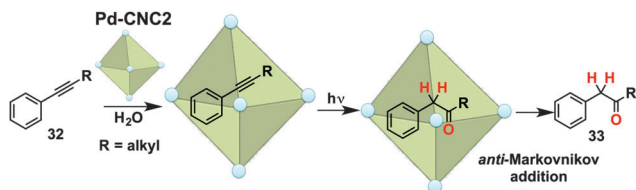
4.4. Co-ordination nanocages

The interplay between co-ordination chemistry and supramolecular chemistry was cleverly utilized by various groups[46] to build water-soluble co-ordination nanocages (CNCs; Fig. 1) that served as molecular reaction flasks for chemical transformations.[11] We will just highlight one such reaction flask pioneered by Fujita and co-workers[11–13] where they employed capping ligands such as ethylenediamine derivatives to enforce the 90° *cis*-geometry around square-planar coordinated Pd[II] and Pt[II] ions. By mixing these end-capped metal ions with the tridentate, triangular ligands such as 1,3,5-tris(4-pyridyl)triazine, self-assembled co-ordination cages (CNC) were synthesized and utilized as molecular reaction flasks. The architecture of CNCs built with triazine ligands as walls of the co-ordination cages that were anchored by metal ions at the corners of the octahedron is shown in Fig. 1. This created a unique structural feature with a cavity that could be employed for confinement and catalysis.

Fujita and co-workers reported highly stereoselective [2+2]-photodimerization of acenaphthylenes 25 in the presence of self-assembled Pd-nanocage Pd-CNC1 (Fig. 1; Scheme 11).[12] They observed the *syn*-HT dimers as the exclusive photoproduct (>98% yield) upon irradiation (3 h) of acenaphthylenes 25a–b in the presence of Pd-CNC1. The reaction was found to be very
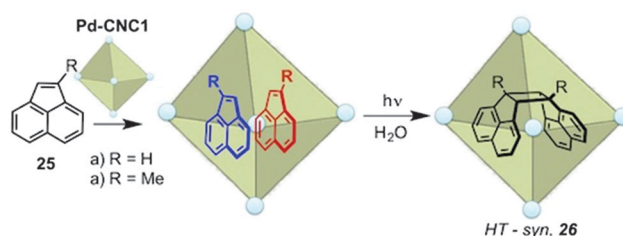
Scheme 11 Stereoselective intermolecular photodimerization of acenaphthylenes in presence of co-ordination nanocage (CNC).

Scheme 12 Photohydration reaction of arylalkyne in the presence of a catalytic amount of coordination nanocage (CNC) leading to an anti-Markovnikov photoproduct.

Scheme 13 Enantioselective intramolecular [2+2]-photocycloaddition reaction of substituted 2-quinolone **34**.

effective with no observable decomposition of CNC during the course of the photoreaction. In the absence of the cage, no reaction was observed for similar irradiation times, while a 1:1 mixture of *syn* (19%) and *anti* (17%) dimers was observed at high concentrations of acenaphthylene **25**. While again not catalytic, this study demonstrated that CNCs were viable molecular flasks that sequestered and pre-oriented two substrates in close proximity thereby promoting dimerization of olefins in a selective fashion.

Building on this precedence, photo-induced hydration of internal arylalkynes with catalytic amounts of CNCs was reported by Fujita and co-workers (Scheme 12).[13] Photoirradiation of 1-phenyl-1-hexyne (**32**, 20 equiv.) in the presence of Pd-nanocage Pd-CNC2 (Fig. 1; Scheme 12) gave the anti-Markovnikov hydration product **33** (benzyl ketone) exclusively through an electron transfer mechanism. The electron transfer occurred from the alkyne to the electron-deficient CNC generating a highly active phenyl alkyne radical cation intermediate. This radical cation intermediate reacted with a water molecule (from the solvent) regioselectively to generate the stabilized benzylic radical resulting in the anti-Markovnikov hydration product. The nanocage also served as a UV-filter for the photoproduct thereby preventing the benzyl ketone photoproduct from further photochemical transformations (α-cleavage/hydrogen abstraction reactions that are expected from the photoproduct).

### 4.5. Sensitizing H-bonding templates for supramolecular photocatalysis

We have seen in the previous sections that confining substrates within molecular flasks/nano-containers can efficiently enhance photochemical reactivity and selectivity. One can also extend this strategy to molecular templates that anchor substrates through non-covalent interactions (*e.g.* H-bonding interactions) to enhance reactivity and selectivity during photochemical transformations. Additionally, by incorporating an asymmetric unit into these templates, stereodifferentiation can be achieved in the photoproduct due to the chiral environment presented by the template. This aspect is quite appealing to chemists across disciplines as it provides a strategy to achieve stereoselectivity in small chiral molecules during photoreactions that is quite challenging. The general design adopted by chemists is to design a hydrogen-bonding template (Fig. 1; Schemes 13–16) that is appended with a sensitizer to enable energy transfer or electron transfer to a reactive substrate and enhance chemical reactivity/selectivity in light initiated reactions. The H-bonding
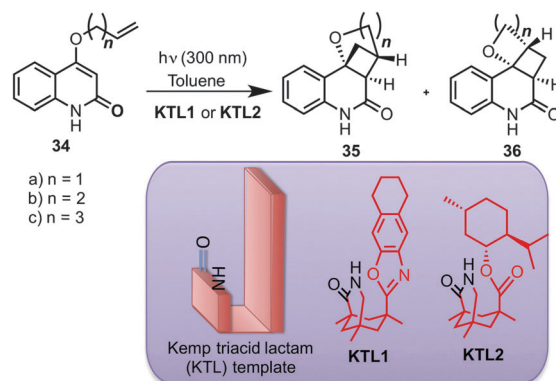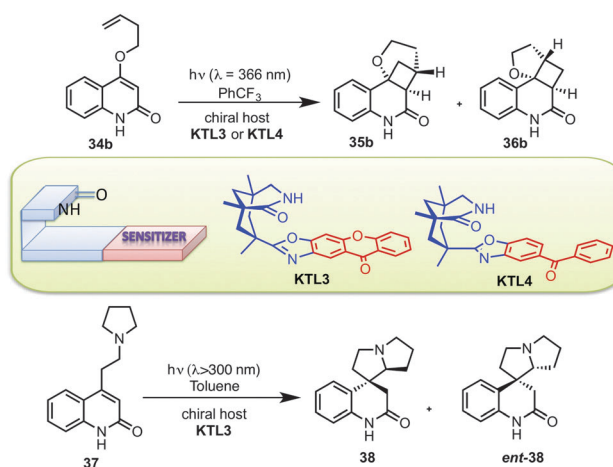
Scheme 14 Enantioselective intramolecular 2+2 photocycloaddition sensitized by a chiral template. Top: energy transfer sensitization of quinolones **34b**. Bottom: electron transfer sensitization of quinolone **37**.
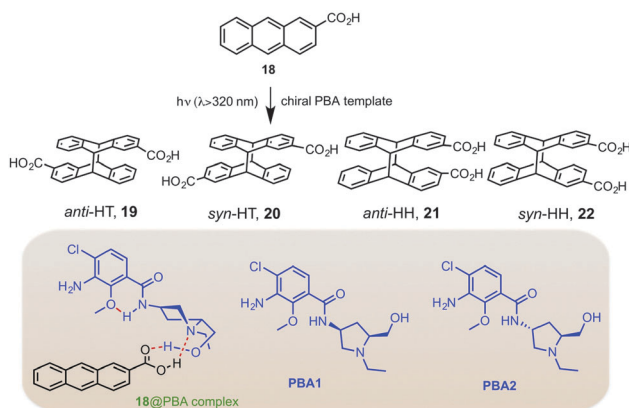
Scheme 15 [4+4]-Photocyclodimerization of 2-anthracenecarboxylate **18** in the presence of a pyrrolidinyl benzamide (PBA) template.

interactions serve as a glue to bring the reactive substrate closer to the sensitizer to enable energy/electron transfer and the architecture of the template enables for facial/stereo-differentiation in the reaction of interest.[3]

Scheme 16 [2+2]-Photocycloaddition of quinolone **34** in the presence of a pyridine-isophthalamide (PIT) template.

Bach and co-workers reported the [2+2]-photocycloaddition reactions of 4-substituted-2-quinolone **34** with Kemp triacid lactam templates (+)-KTL1 and (−)-KTL2 (Scheme 13).[14] Low selectivity observed in the photoproduct **35a** (37% ee, 89% yield, −15 °C) with the (−)-KTL2 host was rationalized due to the weak association between **34a** and the H-bonding template with the menthol ring that led to a lack of stereo-discrimination. However with 2.6 equivalents of (+)-KTL1 high enantioselectivity (93% ee, 77% yield at −60 °C) was observed in **35a**. The photoreaction was also carried out with quinolone **34c** (with a longer alkyl chain) with 1.2 equivalents of chiral host (+)-KTL1 in toluene at −15 °C. High enantioselectivity (88% ee, 88% yield) was observed in the photoproduct **36c**. While not catalytic, this report showed that enantiotopic faces of the photoreactive substrates can be discriminated using Kemp triacid based chiral lactam hosts through hydrogen bonding.

To extend the methodology for catalytic turnover, the chiral Kemp lactam templates were appended with triplet sensitizers to enable energy transfer (Scheme 14).[15,16] Kemp lactam host KTL3 with a xanthone sensitizer and KTL4 with a benzophenone sensitizer were evaluated for intramolecular [2+2]-photocycloaddition of quinolone **34b** (Scheme 14). Under low catalytic loading of KTL4 (10 mol%) low enantioselectivity (39% ee) was observed in photoproduct **36b** at −25 °C in trifluorotoluene. Replacing the benzophenone moiety in KTL4 with xanthone as the triplet sensitizer in KTL3 (Scheme 14) resulted in high enantioselectivity (90% ee with 5 mol% catalytic loading of KTL3) in the photoproduct **36b**. Enantioselectivity increased with an increase in catalyst loading from 5 to 20 mol% with 94% ee value (78% yield). The regiomeric ratio of photoproducts **36b**:**35b** was 79:21. The low efficiency with benzophenone compared to xanthone appended KTL templates was attributed to the absorptivity (optical density at the irradiating wavelengths) and low triplet energy of benzophenone when compared to xanthone.

The use of chiral sensitizers appended to the Kemp lactam host was also extended to electron transfer mediated photo transformation. Benzophenone appended Kemp lactam host KTL4 mediated a photoinduced electron transfer reaction (PET) with quinolone **37** (Scheme 14 bottom).[17] High enantioselectivity (70% ee, 64% yield, 1 h irradiation) was achieved in the photoproduct **38** with catalytic amounts (0.3 eq.) of benzophenone appended Kemp lactam host KTL4 in toluene at −60 °C. The observed selectivity was rationalized by two-point hydrogen bonding to substrate and KTL4 as well as the ability of benzophenone moiety that served as a sensitizer for electron transfer reaction. In addition, the benzophenone appended template

provided the necessary shielding for enantiofacial differentiation during the photochemical transformation.[17]

After successfully employing cyclodextrins as supramolecular hosts for mediating the photocyclodimerization of **18** (Scheme 7),[43] Inoue and co-workers reported enantioselective photocyclodimerization of **18** in the presence of a chiral pyrrolidinyl benzamide (PBA) that served as a H-bonding template (Scheme 15).[18] The pyrrolidinyl benzamide templates PBA1 and PBA2 provided two-point hydrogen bonding sites through the amide and primary alcohol functionalities. Irradiation of **18** in the presence of a PBA template in dichloromethane at two different temperatures (25 °C and −50 °C) yielded photoproducts **19–22** with preferential formation of anti-HT **19** and anti-HH **21** at −50 °C. A significant difference in the ee values was observed in the chiral photoproducts syn-HT **20** and anti-HH **21** in the presence of PBA1 and PBA2. Poor enantiomeric excess (<3% ee) was observed in photoproducts in the presence of a PBA2 template (trans geometry between amide and alcohol functionality). On the other hand, the PBA1 template (cis geometry between amide and alcohol functionality) gave an ee value of 25–43% for syn-HT **20** and an ee value of 10–43% for anti-HH **21** depending on the temperature (25 °C and −50 °C). The enhanced selectivity in the photoproducts was rationalized due to differences in the steric shielding/stereofacial differentiation provided by two templates (PBA1 and PBA2) upon interaction with **18**.

Krische and co-workers[19] reported the use of a chiral pyridine-isophthalamide (PIT) template appended with benzophenone serving as a triplet sensitizer for enantioselective [2+2]-photocycloaddition reaction of quinolones **34b** (Scheme 16). Irradiation of quinolone **34b** with 0.25–2 equivalents of the PIT template in CDCl₃ at −70 °C resulted in an increased efficiency of the photoreaction. However ee values (20% ee) were unaffected in the photoproduct **36b** under sub-stoichiometric or stoichiometric loading levels of the PIT template. This was rationalized based on the intrinsic enantiofacial bias in the host–guest complex formed between the PIT template and the substrate **34b**.

Bassani and co-workers[20,21] reported [2+2]-photodimerization of cinnamate ester **39** covalently functionalized with diaminotriazine (Scheme 17). Barbiturate (BAR) acted as a molecular scaffold recognizing the diaminotriazine functionality thereby pre-orienting the cinnamate ester to increase reactivity and selectivity in the photoproduct. NMR binding experiment showed strong hydrogen bonding between the BAR template and **39** with binding constants $K_1 = 620$ M⁻¹ and $K_2 = 410$ M⁻¹ (1:2 host–guest binding isotherm curve). In the absence of the BAR template, **39** underwent double bond photoisomerization (λ ∼ 350 nm) in dichloromethane leading to a Z:E ratio of 2:1 along with the formation of cyclobutane dimers. Formation of cyclobutane dimers was observed only upon prolonged irradiation. However, irradiation of **39** in the presence of 0.5 equivalents of the BAR template gave photoproducts **40–42**. The regiochemistry in the photoproducts **40–42** was rationalized based on the orientation of the reacting cinnamate chromophore that was dictated by the BAR template. The formation of the ternary complex between the BAR template and two E-**39** molecules
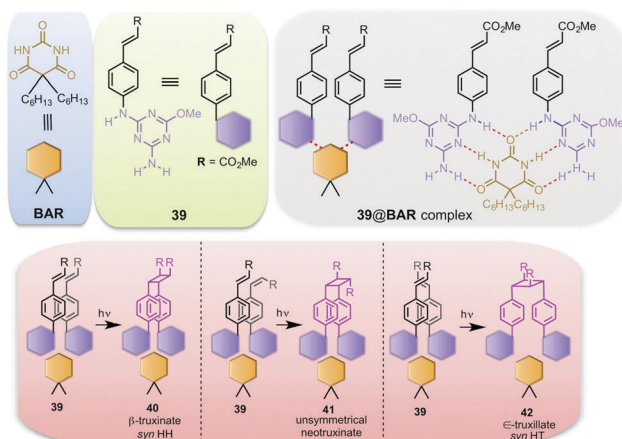
Scheme 17 [2+2]-Photodimerization of cinnamates in the presence of a supramolecular hydrogen-bonded assembly.

with face-to-face orientation yielded β-truxinate isomer **40**, whereas the face-to-face orientation of one *E*-**39** and one *Z*-**39** yielded unsymmetrical neotruxinate isomer **41**. The ∈-truxillate dimer **42** was formed when the double bonds in the two *E*-**39** molecules were crossed due to supramolecular complexation with the BAR template.

4.6. Combining supramolecular assemblies to enhance reactivity and selectivity

To improve the role of confining environments in controlling light initiated processes, the use of two or more assemblies in unison has been shown to be effective. Kim, Inoue, and co-workers[47] reported the [4+4]-photocycloaddition of α-CD functionalized with an anthracene carboxylic acid at the 6-position through an ester linkage *viz.*, 6-*O*-(2-anthracenecarbonyl)-α-CD **43**, (Scheme 18). Substrate **43** functionalized α-CD was templated within either γ-CD or CB[8] and the photodimerization efficiency and selectivity were investigated. The α-CD functionality in **43** served as a bulky hydrophilic substituent and dictated the mode of binding of the anthracene motif inside the supramolecular cavity of both CB[8] and γ-CD that was reflected in the dramatic inversion of the HH : HT ratio at −20 °C at 210 MPa. The *syn*-HT **46** was observed as the major photoproduct in the case of γ-CD with a HH : HT product ratio of 2 : 98 (Scheme 18).
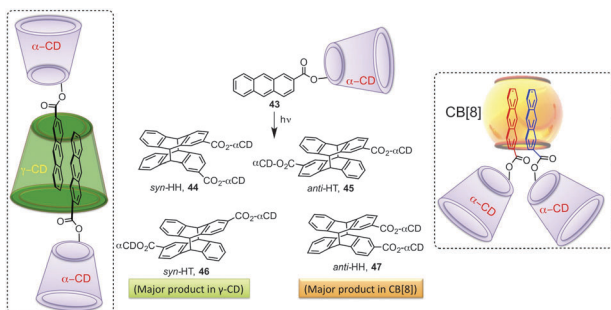
On the other hand, *anti*-HH **47** was observed as the major product with CB[8] with a HH : HT ratio of 99 : 1. The α-CD chiral auxiliary was removed by base hydrolysis to access the optically enriched parent dimers. The photoreactivity with γ-CD gave a 91% ee value in the hydrolyzed *syn*-HT dimer and a 2% ee value in the hydrolyzed *anti*-HH dimer at −20 °C and 210 MPa. On the other hand, in the case of CB[8] at −20 °C at 210 MPa the ee values of 18 and 8% were observed for the hydrolyzed *syn*-HT and *anti*-HH dimers, respectively.

4.7. Photocatalysis mediated by metallosupramolecular assemblies

Inoue and co-workers[22] also cleverly exploited the use of supramolecular host–guest chemistry and metal-mediated photochemistry to control both the enantio-differentiation of substrates within a chiral host and accelerate the photoreaction without using a sensitizer. They functionalized γ-CD at the 6-position with diamino substituents (DA-γ-CD) and evaluated their role in promoting the photodimerization of anthracene carboxylic acid **18** in the presence of Cu(II) ions (Scheme 19). In the presence of Cu(II) ions, DA-γ-CD oriented the two anthracene carboxylic acid molecules in a HH fashion which led to the formation of the optically active *anti*-HH dimer **21**. Photoirradiation of **18** in the presence of 0.1 equivalents of DA-γ-CD and 0.5 equivalents of Cu(II) ions resulted in an ee value of 70% in the *anti*-HH dimer **21**. An ee value of 43% in the *anti*-HH dimer **21** was observed upon decreasing the loading level of DA-γ-CD. Thus the metallosupramolecular photocatalysis was established as an effective alternative to hosts/templates appended with sensitizers (electron/energy transfer sensitizers).

Dictating photochemical reactivity through metal ion complexation has been cleverly exploited by sequestering them using molecular recognition motifs (*e.g.* crown ethers). Saltiel and co-workers reported[24] the intermolecular [2+2]-photocycloaddition of supramolecular assembly **50** formed from **48** and **49** (Scheme 20). The self-assembled **50** was stabilized by hydrogen bonding, π–π interactions and sandwich Ba^{+2} complex formation between crown ether units in **48** and **49**. These non-bonding interactions oriented the double bonds at an optimal distance for photochemical dimerization that occurred effectively
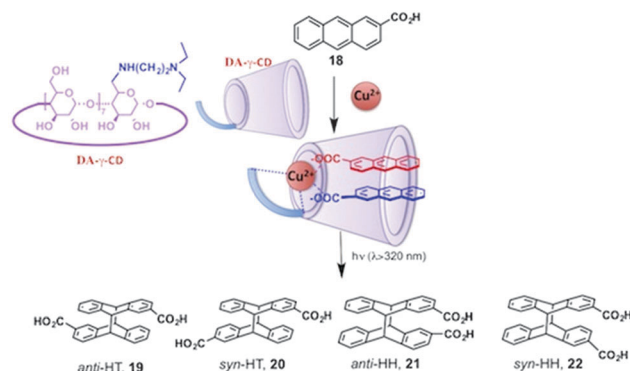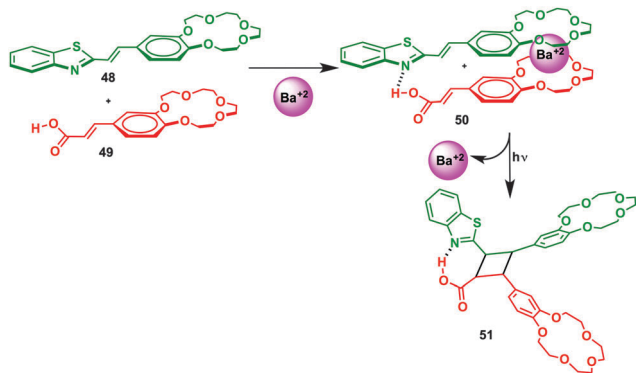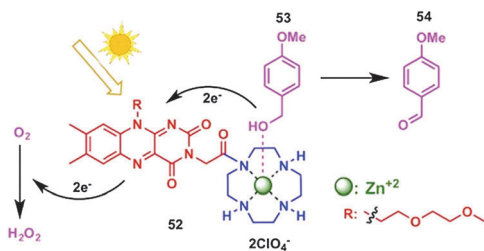

Scheme 18 Combining supramolecular assemblies to influence excited state chemistry of cyclodextrin-appended anthracene carboxylic acid derivative **43**.

Scheme 19 Metallosupramolecular photodimerization of **18** mediated by diamino functionalized γ-CD derivatives (DA-γ-CD) in the presence of Cu(ClO$_4$)$_2$ in aqueous methanol.

This journal is © The Royal Society of Chemistry 2014

Chem. Soc. Rev., 2014, **43**, 4084–4101 | **4097**

Scheme 20 Metallosupramolecular photochemistry: intermolecular [2+2]-photocycloaddition of supramolecular assembly **50** anchored by Ba²⁺ leading to formation of unsymmetrical cycloadduct **51**.

Scheme 21 Catalytic photooxidation of benzyl alcohol **53** to benzaldehyde **54** mediated by the flavin–zinc(II)–cyclen complex **52** in the presence of oxygen.

in the presence of Ba²⁺ ions leading to the formation of unsymmetrical cyclobutane adduct **51**. The report highlights the importance of preorganization of substrates in the presence of metal cation(s) that controlled photocycloaddition in solution leading to the exclusive formation of cyclobutane **51** in high yields.

König and co-workers[23] demonstrated the use of metallosupramolecular assembly to perform catalytic photooxidation of benzyl alcohol **53** to benzaldehyde **54** using a flavin containing template **52** (Scheme 21) that featured a zinc recognition site (zinc(II)–cyclen). Flavin acted as a light absorbing chromophore that initiated an intramolecular photoinduced electron transfer from coordinated benzyl alcohol **53** to the excited flavin chromophore unit producing the benzaldehyde product **54** and the photo-reduced flavin **52**. The reduced flavin was then reoxidized by air (oxygen) regenerating the flavin chromophore in **52** rendering the template catalytic. The reaction worked efficiently in both acetonitrile ($\phi = 3.8 \times 10^{-2}$; turnover number = 20) and water ($\phi = 0.4$). However, in the absence of template **52** there was no observable product formation. The reaction was efficient with quantum yields 30 times higher than the intermolecular process. The study demonstrates the importance of combination of a photosensitizer (flavin) and a substrate in proximity for efficient photochemical transformations.

4.8. Supramolecular photocatalysis assisted by mechanical grinding

While efficient dynamic exchange of reactants and products is critical for supramolecular catalysis in solution, tailoring the

thermodynamic and kinetic aspects to achieve such an exchange is often time challenging. Employing supramolecular confinement in the solid-state offers avenues to overcome many of the problems faced in solution phase reactivity. Controlling reaction rates in the solid state via crystal engineering is very attractive as the slow diffusion limits the number of unwanted side reactions that are often encountered during light induced processes. This also provides an opportunity to use mechanical force to alter the supramolecular arrangement in addition to promoting/altering the orientation of guest molecule(s). Further, the mechanical force can be utilized as a tool for exchanging the reactants and the photoproducts with the supramolecular host. The strategy involves mechanical grinding of the photoactive reactants with templates/additives for enhancing the reactivity leading to photoproducts. After irradiation, the molecular templates are recycled by re-grinding the solid-state mixture allowing the supramolecular template/additives bind to other reactants (exchanging the reactant and the product with the supramolecular host by mechanical force) facilitating the photochemical transformation in a sustainable manner. This process is attractive as the phototransformation is done under solvent free conditions.

Mechanical grinding of cucurbit[8]uril (CB[8]; 50 mol%) or other additives (e.g. thiourea or adamantine) with 6-methylcoumarin **10** resulted in an enhanced photodimerization efficiency with exclusive formation of head-to-head photodimer **11** (Scheme 22).[48] A red shift in the fluorescence of **10** was observed in the solid-state upon mechanical grinding with CB[8]. This red shift in fluorescence was similar to the red-shifted fluorescence emission observed for the CB[8]–**10** host–guest complex in solution at 298 K (Fig. 6-top).[39,48] Phosphorescence emission observed in the solid state for mechanically ground **10** with CB[8] at 77 K was similar to the phosphorescence profile observed for the **10**@CB[8] host–guest complex at 77 K (Fig. 6-bottom).[39,48] The single crystal X-ray structure of **10** revealed a head-to-head orientation of coumarins with the distance between the double bonds being 4.695 Å that resulted in no observable photodimerization even after 200 h of irradiation.[49] Control studies in the presence of H-bonding thiourea as an additive gave syn-HH **11** exclusively. Control studies by grinding **10** alone also resulted in similar conversions. The reactivity of **10** upon mechanical grinding was in contrast to the reported behavior[49] for photodimerization in the solid state. Enhancement of
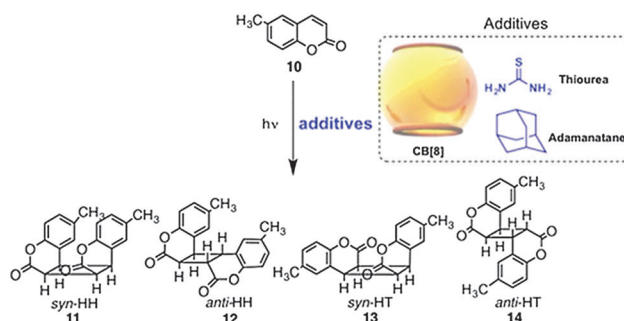
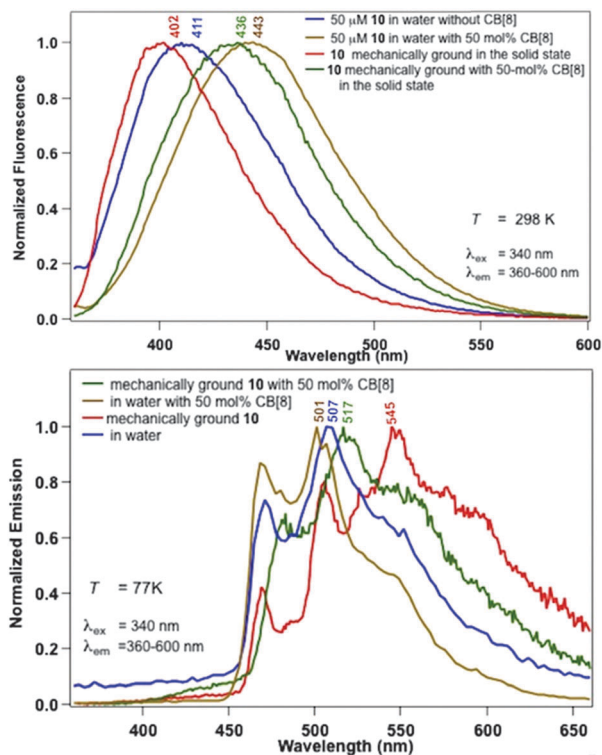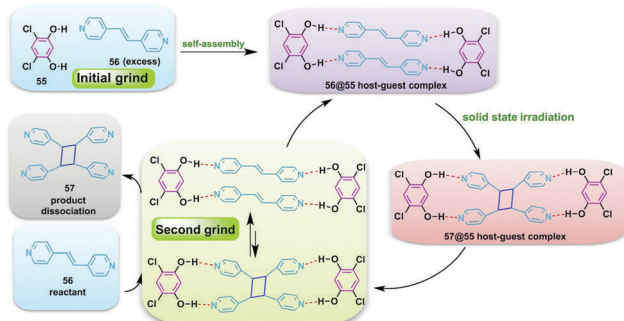**Scheme 22** Photodimerization of 6-methylcoumarin catalyzed by CB[8].

Fig. 6 (top) Normalized emission of **10** in the presence and absence of CB[8] in water and in the solid-state at 298 K. (bottom) Normalized emission spectra of **10** in the presence and absence of CB[8] in water and in the solid-state at 77 K. Adapted from ref. 48 and reproduced with permission of Elsevier.

photoreactivity of **10** upon mechanical grinding was rationalized due to a combination of factors, *viz.*: (a) crystalline imperfection/defects that are likely formed during mechanical grinding and/or; (b) formation of a new amorphous phase due to mechanical grinding was not ruled out by powder XRD analysis.

One of the best examples of promoting photoreactivity through mechanical grinding by adding catalytic amounts of additives/supramolecular receptor(s) in the solid state was reported by MacGillivray and co-workers (Scheme 23).[50] They investigated the [2+2]-photodimerization of *trans*-1,2-bis(4-pyridyl)ethylene (DPE) **56** in the solid state by employing 4,6-dichloro-resorcinol

Scheme 23 Solid-state [2+2]-photodimerization of BPE in the presence of a ditopic H-bonding host DCR **55** through mechanical grinding.

(DCR) **55** as a ditopic supramolecular catalyst through mechanical grinding.[50] Irradiation of **56** in the presence of **55** (20 mol%) gave a dimerized photoproduct rctt-tetrakis(4-pyridyl) cyclobutane (4,4′-tpcb) **57** in quantitative yields. In order to achieve turnover in the absence of solvent, the reaction was performed through dry mechanical grinding. The initial grinding between catalyst **55** and reactant **56** resulted in the formation of a reactive **56@55** host–guest complex (hydrogen bonded complex) that reacted efficiently due to the closer double bond distance (Scheme 23) to form the photoproduct **57**. The photoproduct **57** formed was bound to the catalyst **55**. The key step involved a second grinding where the receptor (catalyst **55**) dissociated from the photoproduct **57**. During the second grinding the photoproduct **57** efficiently dissociated from the catalyst **55** due to the release of strain from the photoproduct–catalyst complex. The free catalyst **55** then templated unreacted substrates enhancing their photoreactivity and turnover. The photoproduct **57** was observed exclusively with good yields when sub-stoichiometric amounts (10, 20 and 50 mol%) of **55** were employed. This report demonstrated an elegant way of combining supramolecular photocatalysis and mechanical stimuli to control and promote photochemical transformations.

5 Some guidelines to follow while designing supramolecular photocatalytic systems

To develop supramolecular photocatalytic systems it is critical to have a thorough understanding of not only the photochemical and photophysical aspects of the chromophore under investigation within confined and isotropic media but also a good understanding of the physical organic parameters involved in the system *viz.*, thermodynamic binding constant(s), kinetic rate constants, reaction velocity/quantum yield of the photoreaction to name a few. While the criteria and the specific needs for every reaction will be different in terms of its reaction conditions, few of the fundamental aspects needs to be satisfied. Irrespective of the type of host–guest complex(s)/supramolecular system, a clear understanding of supramolecular host–guest interactions reflected by the thermodynamic binding constants of the reactant(s) and the photoproduct(s) is necessary. As the system needs to undergo catalytic turnover, the system needs to be dynamic with the binding affinity of the reactive guest(s) being greater or at the very least comparable to the binding affinity of the photoproduct(s) to prevent product inhibition during the catalytic processes. To appreciate the turnover involved in the photocatalytic cycle, the kinetics of the individual microscopic steps (both forward and reverse rate constants) needs to be established. Finally, the efficiency of the photochemical transformation mediated by the supramolecular host needs to be quantified through reaction velocity measurements or quantum yield studies. Together, these parameters will provide a clear picture of how supramolecular interactions control reactivity leading to photocatalysis in the system of interest.

This journal is © The Royal Society of Chemistry 2014

Chem. Soc. Rev., 2014, **43**, 4084–4101 | **4099**

6 Future outlook

Designing and synthesizing supramolecular scaffolds have provided chemists with the ability to control both thermal and photochemical reactions. Understanding the functional features of supramolecular systems will provide opportunities to develop the field of supramolecular catalysis with programmed control over reactivity and product selectivity. In particular controlling and catalyzing light induced transformations require not only an intricate understanding of thermodynamic and kinetic aspects of host–guest complexation but also a clear understanding of excited state processes. Tailoring supramolecular interactions with well-defined roles to promote and control photochemical reactions will open up exciting prospects that are not observed in conventional chemical systems.

Acknowledgements

Notes and references

1 R. Breslow, *Acc. Chem. Res.*, 1995, **28**, 146–153.
2 D. M. Vriezema, A. M. Comellas, J. A. A. W. Elemans, J. J. L. M. Cornelissen, A. E. Rowan and R. J. M. Nolte, *Chem. Rev.*, 2005, **105**, 1445–1490.
3 J. Svoboda and B. König, *Chem. Rev.*, 2006, **106**, 5413–5430.
4 B. C. Pemberton, R. Raghunathan, S. Volla and J. Sivaguru, *Chem. – Eur. J.*, 2012, **18**, 12178–12190.
5 J. Sivaguru, A. Natarajan, L. S. Kaanumalle, J. Shailaja, S. Uppili, A. Joy and V. Ramamurthy, *Acc. Chem. Res.*, 2003, **36**, 509–521.
6 R. Behrend, E. Meyer and F. Rusche, *Liebigs Ann. Chem.*, 1905, **339**, 1–37.
7 J. W. Lee, S. Samal, N. Selvapalam, H.-J. Kim and K. Kim, *Acc. Chem. Res.*, 2003, **36**, 621–630.
8 E. Masson, X. Ling, R. Joseph, L. Kyeremeh-Mensah and X. Lu, *RSC Adv.*, 2012, **2**, 1213–1247.
9 J. Szejtli, *Chem. Rev.*, 1998, **98**, 1743–1754.
10 C. L. D. Gibb and B. C. Gibb, *J. Am. Chem. Soc.*, 2004, **126**, 11408–11409.
11 M. Yoshizawa, J. K. Klosterman and M. Fujita, *Angew. Chem., Int. Ed.*, 2009, **48**, 3418–3438.
12 M. Yoshizawa, Y. Takeyama, T. Kusukawa and M. Fujita, *Angew. Chem., Int. Ed.*, 2002, **41**, 1347–1349.
13 T. Murase, H. Takezawa and M. Fujita, *Chem. Commun.*, 2011, **47**, 10960–10962.
14 T. Bach, H. Bergmann and K. Harms, *Angew. Chem., Int. Ed.*, 2000, **39**, 2302–2304.
15 C. Müller, A. Bauer and T. Bach, *Angew. Chem., Int. Ed.*, 2009, **48**, 6640–6642.
16 C. Müller, A. Bauer, M. M. Maturi, M. C. Cuquerella, M. A. Miranda and T. Bach, *J. Am. Chem. Soc.*, 2011, **133**, 16689–16697.
17 A. Bauer, F. Westkamper, S. Grimme and T. Bach, *Nature*, 2005, **436**, 1139–1140.
18 J.-i. Mizoguchi, Y. Kawanami, T. Wada, K. Kodama, K. Anzai, T. Yanagi and Y. Inoue, *Org. Lett.*, 2006, **8**, 6051–6054.
19 D. F. Cauble, V. Lynch and M. J. Krische, *J. Org. Chem.*, 2003, **68**, 15–21.
20 D. M. Bassani, V. Darcos, S. Mahony and J.-P. Desvergne, *J. Am. Chem. Soc.*, 2000, **122**, 8795–8796.
21 V. Darcos, K. Griffith, X. Sallenave, J.-P. Desvergne, C. Guyard-Duhayon, B. Hasenknopf and D. M. Bassani, *Photochem. Photobiol. Sci.*, 2003, **2**, 1152–1161.
22 C. Ke, C. Yang, T. Mori, T. Wada, Y. Liu and Y. Inoue, *Angew. Chem., Int. Ed.*, 2009, **48**, 6675–6677.
23 R. Cibulka, R. Vasold and B. König, *Chem. – Eur. J.*, 2004, **10**, 6223–6231.
24 O. Fedorova, Y. V. Fedorov, E. Gulakova, N. Schepel, M. Alfimov, U. Goli and J. Saltiel, *Photochem. Photobiol. Sci.*, 2007, **6**, 1097–1105.
25 C. Yang and Y. Inoue, *Chem. Soc. Rev.*, 2014, DOI: 10.1039/C3CS60339C.
26 B. Bibal, C. Mongin and D. M. Bassani, *Chem. Soc. Rev.*, 2014, DOI: 10.1039/C3CS60366K.
27 L. S. Kaanumalle and V. Ramamurthy, *Chem. Commun.*, 2007, 1062–1064.
28 R. Kulasekharan, M. V. S. N. Maddipatla, A. Parthasarathy and V. Ramamurthy, *J. Org. Chem.*, 2013, **78**, 942–949.
29 K. A. Connors, *Binding Constants*, John Wiley, New York, 1987.
30 W. A. Freeman, W. L. Mock and N.-Y. Shih, *J. Am. Chem. Soc.*, 1981, **103**, 7367–7368.
31 J. Kim, I.-S. Jung, S.-Y. Kim, E. Lee, J.-K. Kang, S. Sakamoto, K. Yamaguchi and K. Kim, *J. Am. Chem. Soc.*, 2000, **122**, 540–541.
32 A. Day, A. P. Arnold, R. J. Blanch and B. Snushall, *J. Org. Chem.*, 2001, **66**, 8094–8100.
33 *Special issue on Cucurbituils*, Israel Journal of Chemistry, WILEY-VCH Verlag, 2011.
34 S. Y. Jon, Y. H. Ko, S. H. Park, H.-J. Kim and K. Kim, *Chem. Commun.*, 2001, 1938–1939.
35 M. Pattabiraman, A. Natarajan, R. Kaliappan, J. T. Mague and V. Ramamurthy, *Chem. Commun.*, 2005, 4542–4544.
36 M. V. S. N. Maddipatla, L. S. Kaanumalle, A. Natarajan, M. Pattabiraman and V. Ramamurthy, *Langmuir*, 2007, **23**, 7545–7554.
37 R. Wang, L. Yuan and D. H. Macartney, *J. Org. Chem.*, 2006, **71**, 1237–1239.
38 B. C. Pemberton, N. Barooah, D. K. Srivatsava and J. Sivaguru, *Chem. Commun.*, 2010, **46**, 225–227.
39 B. C. Pemberton, E. Kumarasamy, S. Jockusch, D. K. Srivastava and J. Sivaguru, *Can. J. Chem.*, 2011, **89**, 310–316.
40 B. C. Pemberton, R. K. Singh, A. C. Johnson, S. Jockusch, S. J. P. Da, A. Ugrinov, N. J. Turro, D. K. Srivastava and J. Sivaguru, *Chem. Commun.*, 2011, **47**, 6323–6325.

4100 | *Chem. Soc. Rev.*, 2014, **43**, 4084–4101

This journal is © The Royal Society of Chemistry 2014

41 B. C. Pemberton, PhD thesis, North Dakota State University, 2012.

42 W. S. Chung, N. J. Turro, J. Silver and W. J. Le Noble, *J. Am. Chem. Soc.*, 1990, **112**, 1202–1205.

43 A. Nakamura and Y. Inoue, *J. Am. Chem. Soc.*, 2003, **125**, 966–972.

44 Y. Inoue, T. Wada, N. Sugahara, K. Yamamoto, K. Kimura, L.-H. Tong, X.-M. Gao, Z.-J. Hou and Y. Liu, *J. Org. Chem.*, 2000, **65**, 8041–8050.

45 P. Jagadesan, B. Mondal, A. Parthasarathy, V. J. Rao and V. Ramamurthy, *Org. Lett.*, 2013, **15**, 1326–1329.

46 T. R. Cook, Y.-R. Zheng and P. J. Stang, *Chem. Rev.*, 2012, **113**, 734–777.

47 C. Yang, T. Mori, Y. Origane, Y. H. Ko, N. Selvapalam, K. Kim and Y. Inoue, *J. Am. Chem. Soc.*, 2008, **130**, 8574–8575.

48 B. C. Pemberton, A. Ugrinov and J. Sivaguru, *J. Photochem. Photobiol., A*, 2013, **255**, 10–15.

49 K. Gnanaguru, N. Ramasubbu, K. Venkatesan and V. Ramamurthy, *J. Org. Chem.*, 1985, **50**, 2337–2346.

50 A. N. Sokolov, D.-K. Bučar, J. Baltrusaitis, S. X. Gu and L. R. MacGillivray, *Angew. Chem., Int. Ed.*, 2010, **49**, 4273–4277.